


Efficient Sampling for Gaussian Linear Regression With Arbitrary Priors

P. Richard Hahn, Jingyu He & Hedibert F. Lopes


To cite this article: P. Richard Hahn, Jingyu He & Hedibert F. Lopes (2019) Efficient Sampling for Gaussian Linear Regression With Arbitrary Priors, Journal of Computational and Graphical Statistics, 28:1, 142-154, DOI: [10.1080/10618600.2018.1482762](https://doi.org/10.1080/10618600.2018.1482762)

To link to this article: <https://doi.org/10.1080/10618600.2018.1482762>

 View supplementary material [↗](#)

 Accepted author version posted online: 14 Jun 2018.
Published online: 07 Sep 2018.

 Submit your article to this journal [↗](#)

 Article views: 132

 View Crossmark data [↗](#)



Efficient Sampling for Gaussian Linear Regression With Arbitrary Priors

P. Richard Hahn^a, Jingyu He^b, and Hedibert F. Lopes^c

^aSchool of Mathematical and Statistical Sciences, Arizona State University, Tempe, AZ, ^bBooth School of Business, University of Chicago, Chicago, IL; ^cINSPER Institute of Education and Research, Sao Paulo, Brazil

ABSTRACT

This article develops a slice sampler for Bayesian linear regression models with arbitrary priors. The new sampler has two advantages over current approaches. One, it is faster than many custom implementations that rely on auxiliary latent variables, if the number of regressors is large. Two, it can be used with any prior with a density function that can be evaluated up to a normalizing constant, making it ideal for investigating the properties of new shrinkage priors without having to develop custom sampling algorithms. The new sampler takes advantage of the special structure of the linear regression likelihood, allowing it to produce better effective sample size per second than common alternative approaches.

ARTICLE HISTORY

Received August 2016
Revised May 2018

KEYWORDS

Bayesian computation;
Linear regression; Shrinkage
priors; Slice sampling

1. Introduction

This article develops a computationally efficient posterior sampling algorithm for Bayesian linear regression models with Gaussian errors. Our new approach is motivated by the fact that existing software implementations for Bayesian linear regression do not readily handle problems with large number of observations (hundreds of thousands) and predictors (thousands). Moreover, existing sampling algorithms for popular shrinkage priors are bespoke Gibbs samplers based on case-specific latent variable representations. By contrast, the new algorithm does not rely on case-specific auxiliary variable representations, which allows for rapid prototyping of novel shrinkage priors outside the conditionally Gaussian framework.

Specifically, we propose a slice-within-Gibbs sampler based on the elliptical slice sampler of Murray, Adams, and MacKay (2010). These authors focus on sampling from posteriors that are proportional to a product of a multivariate Gaussian prior and an arbitrary likelihood. Intuitively, the elliptical slice sampler operates by drawing samples from the Gaussian factor of the posterior and then accepting or rejecting these samples by evaluating the non-Gaussian factor. The starting point of this article is the observation that the elliptical slice sampler is also suited to the Bayesian Gaussian linear regression case, which has a multivariate Gaussian likelihood and an arbitrary prior (i.e., the roles of the likelihood and prior are reversed). In fact, under independent priors over the regression coefficients, the Gaussian likelihood term contains all of the co-dependence information of the posterior, allowing us to precompute many key quantities, leading to a remarkably efficient, generic algorithm.

After explaining the new sampler in detail in the following section, extensive computational demonstrations are provided in Section 3. The new sampling approach is demonstrated on the horseshoe prior (Carvalho, Polson, and Scott 2010), the Laplace prior (Park and Casella 2008; Hans 2009), and the

independent Gaussian or “ridge” prior. These three priors boast widely available, user-friendly implementations. Although other shrinkage priors have been proposed and studied, many have not been implemented in the regression setting and hence are not widely used outside of the normal-means context; consequently, we restrict our comparison to three popular regression priors. Recently developed priors that are not considered here include the Dirichlet–Laplace prior (Bhattacharya et al. 2015), the normal-gamma prior (Caron and Doucet 2008; Griffin et al. 2010; Griffin and Brown 2011), the Bayesian bridge (Polson, Scott, and Windle 2014), and many others (Armagan 2009; Polson and Scott 2010; Armagan, Clyde, and Dunson 2011; Armagan, Dunson, and Lee 2013; Neville et al. 2014).

We further demonstrate the flexibility of our approach by using it to perform posterior inference under two nonstandard, “exotic,” priors—an asymmetric Cauchy prior and a “nonlocal” two-component mixture prior—for which there exist no standard samplers. Our approach is also suitable for the case where there are more predictors than observations; in this regime, we compare to Johndrow, Orenstein, and Bhattacharya (2017) whose new Markov chain Monte Carlo algorithm works for tens of thousands of variables. Our method is implemented in C++ as the package `bayeslm` (Hahn, He, and Lopes 2018) in R (R Core Team 2017).

2. Elliptical Slice Sampling for Shrinkage Regression with Arbitrary Priors

2.1. Review of Elliptical Slice Sampling for Gaussian Priors

To begin, we review the elliptical slice sampler of Murray, Adams, and MacKay (2010). In the following subsections, we adapt the sampler specifically for use with Gaussian linear regression models. Unless otherwise noted, random variables

(possibly vector-valued) are denoted by capital Roman letters, matrices are in bold, vectors are in Roman font, and scalars are italic. All vectors are column vectors.

The elliptical slice sampler considers cases where the goal is to sample from a distribution $p(\Delta) \propto N(\Delta; 0, \mathbf{V})L(\Delta)$. The key idea is to take advantage of the elementary fact that the sum of two Gaussian random variables is a Gaussian random variable. Accordingly, for two independent (vector) random variables $v_0 \sim N(0, \mathbf{V})$ and $v_1 \sim N(0, \mathbf{V})$ and for any $\theta \in [0, 2\pi]$, $\Delta = v_0 \sin \theta + v_1 \cos \theta$ is also distributed according to $N(0, \mathbf{V})$, since $\text{cov}(\Delta) = \mathbf{V} \sin^2 \theta + \mathbf{V} \cos^2 \theta = \mathbf{V}$. Because this holds for each θ , the marginal distribution of Δ is $N(0, \mathbf{V})$ for any distribution over θ .

Therefore, Murray, Adams, and MacKay (2010) noted that if one can sample from the parameter-expanded model $p(v_0, v_1, \theta) \propto \pi(\theta)N(v_0; 0, \mathbf{V})N(v_1; 0, \mathbf{V})L(v_0 \sin \theta + v_1 \cos \theta)$, then samples from $p(\Delta)$ can be obtained as samples of the transformation $v_0 \sin \theta + v_1 \cos \theta$. Sampling from this model is easiest to explain in terms of a singular Gaussian prior distribution over $(v_0^t, v_1^t, \Delta^t)^t$ with covariance

$$\Sigma_\theta = \begin{pmatrix} \mathbf{V} & 0 & \mathbf{V} \sin \theta \\ 0 & \mathbf{V} & \mathbf{V} \cos \theta \\ \mathbf{V} \sin \theta & \mathbf{V} \cos \theta & \mathbf{V} \end{pmatrix}$$

and joint density $p(v_0, v_1, \Delta, \theta) \propto N(0, \Sigma_\theta)L(v_0 \sin \theta + v_1 \cos \theta)$. Using this model, we sample the parameters $(v_0, v_1, \Delta, \theta)$ via a two-block Gibbs sampler:

1. Sample from $p(v_0, v_1 | \Delta, \theta)$, which can be achieved by sampling $v \sim N(0, \mathbf{V})$ and setting $v_0 = \Delta \sin \theta + v \cos \theta$ and $v_1 = \Delta \cos \theta - v \sin \theta$.
2. Sample from $p(\Delta, \theta | v_0, v_1) \propto N(0, \Sigma_\theta)L(v_0 \sin \theta + v_1 \cos \theta)$ compositionally in two steps:
 - (a) First draw from $p(\theta | v_0, v_1)$ by marginalizing over Δ , yielding $p(\theta | v_0, v_1) \propto L(v_0 \sin \theta + v_1 \cos \theta)$. We draw from this distribution via a traditional one-dimensional slice sampler (Neal 2003). Initialize $a = 0$ and $b = 2\pi$.
 - i. Draw ℓ uniformly on $[0, L(v_0 \sin \theta + v_1 \cos \theta)]$.
 - ii. Sample θ' uniformly on $\theta \in [a, b]$.
 - iii. If $L(v_0 \sin \theta' + v_1 \cos \theta') > \ell$, set $\theta \leftarrow \theta'$. Otherwise, shrink the support of θ' (if $\theta' < \theta$, set $a \leftarrow \theta'$; if $\theta' > \theta$, set $b \leftarrow \theta'$), and go to step ii.
 - (b) Then we draw from $p(\Delta | \theta, v_0, v_1)$, which is degenerate at $\Delta = v_0 \sin \theta + v_1 \cos \theta$.

Note that this version of the elliptical slice sampler is somewhat different than the versions presented in Murray, Adams, and MacKay (2010), but as it reduces to a Gibbs sampler, its validity is more transparent and practically the algorithms are nearly equivalent.

2.2. Elliptical Slice Sampling for Gaussian Linear Regression

In this section, we adapt the sampler described above to permit efficient sampling from Bayesian linear regression models. Specifically, we consider the standard Bayesian linear regression model:

$$Y = \mathbf{X}\beta + \epsilon, \tag{1}$$

where Y is an n -by-1 vector of responses, \mathbf{X} is an n -by- p matrix of regressors, β is a p -by-1 vector of coefficients, and $\epsilon \sim N(0, \sigma^2 \mathbf{I})$ is an n -by-1 vector of error terms. Denote the prior of β as $\pi(\beta)$. The objective is to sample from a posterior expressible as

$$\pi(\beta | y, \mathbf{X}, \sigma^2) \propto f(y | \mathbf{X}, \beta, \sigma^2 \mathbf{I})\pi(\beta), \tag{2}$$

where $f(y | \mathbf{X}, \beta)$ denotes a multivariate Gaussian density with mean vector $\mathbf{X}\beta$ and diagonal covariance $\sigma^2 \mathbf{I}$. Our approach is driven by the fact that, up to proportionality, this n -dimensional Gaussian can be regarded as the posterior of β under a flat prior (indicated by the 0 subscript):

$$\begin{aligned} \pi_0(\beta | \sigma^2, y, \mathbf{X}) &\propto \frac{1}{\sqrt{2\pi\sigma^2}} \exp\left[-\frac{1}{2\sigma^2}(y - \mathbf{X}\hat{\beta})^T(y - \mathbf{X}\hat{\beta})\right] \\ &\times \frac{1}{\sqrt{2\pi\sigma^2}} \exp\left[-\frac{1}{2\sigma^2}(\beta - \hat{\beta})^T \mathbf{X}^T \mathbf{X}(\beta - \hat{\beta})\right], \end{aligned} \tag{3}$$

which is the density of a p -dimensional Gaussian with mean $\hat{\beta} = (\mathbf{X}^T \mathbf{X})^{-1} \mathbf{X}^T y$ (the ordinary least-square estimate) and covariance $\sigma^2 (\mathbf{X}^T \mathbf{X})^{-1}$. Therefore, the slice sampler of Murray, Adams, and MacKay (2010) can be applied directly, using $\pi_0(\beta | \sigma^2, y, \mathbf{X})$ as the Gaussian ‘‘prior’’ and $\pi(\beta)$ as the ‘‘likelihood.’’ One minor modification is that, because $\pi_0(\beta | \sigma^2, y, \mathbf{X})$ is centered at OLS estimator $\hat{\beta}$, as opposed to 0, we sample the offset of β from $\hat{\beta}$, which we denote $\Delta = \beta - \hat{\beta}$.

This sampler is flexible because the only requirement is that the prior function $\pi(\beta)$ can be evaluated up to a normalizing constant. The sampler is efficient, per iteration, because in each Monte Carlo iteration, the sampler draws a single multivariate Gaussian random variable, and then draws from a univariate uniform distribution within the while loop. The size of the sampling region for θ shrinks rapidly with each rejected value and is guaranteed to eventually accept. Sampling of σ^2 can be done after sampling β in each iteration.

Despite being quite fast per iteration, for larger regression problems, with p having more than a few dozen elements, the autocorrelation from this joint sampler can be prohibitively high, yielding very low effective sample sizes. Intuitively, this occurs because for any given auxiliary variables (v_0, v_1) , the slice step over θ frequently has only a very narrow acceptable region, entailing that subsequent samples of θ (and hence β) will be very close to one another. Fortunately, the basic strategy of the elliptical slice sampler can be applied to smaller blocks, an approach we describe in the following section.

2.3. Elliptical Slice-Within-Gibbs for Linear Regression

As mentioned above, if the number of regression coefficients p is large, the slice which contains acceptable proposals is likely to be minuscule. Due to the shrinking bracket mechanism of the slice sampler, it rejects many proposals and shrinks the bracket strongly toward the initial value, thereby inducing high autocorrelation in the obtained samples. Here, we propose a slice-within-Gibbs sampler (Figure 2) to mitigate this problem.

Because β has a jointly Gaussian likelihood and independent priors, it is natural to implement a Gibbs sampler, updating a subset, which we denote β^k , given all other coefficients, which

Algorithm 1 : *Elliptical slice sampler for linear regression*

For initial value β , with $\Delta = \beta - \hat{\beta}$, and σ^2 fixed:

1. Draw $v \sim N(0, \sigma^2(\mathbf{X}^T \mathbf{X})^{-1})$. Set $v_0 = \Delta \sin \theta + v \cos \theta$ and $v_1 = \Delta \cos \theta - v \sin \theta$.
2. Draw ℓ uniformly on $[0, \pi(\hat{\beta} + v_0 \sin \theta + v_1 \cos \theta)]$. Initialize $a = 0$ and $b = 2\pi$.
 - (a) Sample θ' uniformly on $[a, b]$.
 - (b) If $\pi(\hat{\beta} + v_0 \sin \theta' + v_1 \cos \theta') > \ell$, set $\theta \leftarrow \theta'$ and go to step 3. Otherwise, shrink the support of θ' (if $\theta' < \theta$, set $a \leftarrow \theta'$; if $\theta' > \theta$, set $b \leftarrow \theta'$), and go to step 2(a).
3. Return $\Delta = v_0 \sin \theta + v_1 \cos \theta$ and $\beta = \hat{\beta} + \Delta$.

Figure 1. The elliptical slice sampler for linear regression (with an arbitrary prior) samples all p elements of the regression coefficients simultaneously.

we denote β^{-k} (and other parameters), in each MCMC iteration. This is possible because the conditional distribution for the Gaussian portion of the distribution, which accounts for all the dependence, is well-known and easy to sample from. The basic idea is simply to apply the sampler from [Figure 1](#) using the conditional distribution $\beta^k \mid \beta^{-k}$ as the “likelihood” instead of the full likelihood $L(\beta)$.

From Equation (3), the joint likelihood of β is $N(\hat{\beta}, \sigma^2(\mathbf{X}^T \mathbf{X})^{-1})$. Therefore, we group elements of β into several blocks $\beta = (\beta_1, \dots, \beta_p) = \{\beta^1, \beta^2, \dots, \beta^K\}$, constructing a Gibbs sampling scheme for all K blocks, using the elliptical slice sampler to update each block. We can rearrange terms of the joint distribution as

$$\begin{bmatrix} \beta^k \\ \beta^{-k} \end{bmatrix} \sim N \left(\begin{bmatrix} \hat{\beta}^k \\ \hat{\beta}^{-k} \end{bmatrix}, \sigma^2 \begin{bmatrix} \Sigma_{k,k} & \Sigma_{k,-k} \\ \Sigma_{-k,k} & \Sigma_{-k,-k} \end{bmatrix} \right), \quad (4)$$

where $[\hat{\beta}^k] = \hat{\beta}$, the OLS estimator and $[\Sigma_{k,k} \ \Sigma_{k,-k} \\ \Sigma_{-k,k} \ \Sigma_{-k,-k}] = (\mathbf{X}^T \mathbf{X})^{-1}$.

The corresponding conditional distribution of β^k given β^{-k} is $N(\tilde{\beta}^k, \tilde{\Sigma}^k)$ where

$$\tilde{\beta}^k = \hat{\beta}^k + \Sigma_{k,-k} \Sigma_{-k,-k}^{-1} (\beta^{-k} - \hat{\beta}^{-k}) \quad (5)$$

$$\tilde{\Sigma}^k = \sigma^2 \left(\Sigma_{k,k} - \Sigma_{k,-k} \Sigma_{-k,-k}^{-1} \Sigma_{-k,k} \right). \quad (6)$$

Note that the grouping of coefficients is arbitrary; if all coefficients are grouped in a single block, we recover the original sampler from [Figure 1](#). Empirically, we find that putting each coefficient in a different block so that $K = p$, and updating coefficients one by one, gives excellent performance. Our complete algorithm is given in [Figure 2](#).

2.4. Computational Considerations

Although the slice-within-Gibbs sampler updates the coefficients iteratively, it can be more efficient than Gibbs samplers based on conditionally Gaussian representations because the structure of the slice sampler allows the necessary matrix factorizations and inversions to be precomputed outside the

main Gibbs loop. Specifically, to efficiently compute the K conditional mean vectors and covariance matrices given in expressions (5) and (6), we can precompute $\Sigma_{k,-k} \Sigma_{-k,-k}^{-1}$, $\Sigma_{k,k} - \Sigma_{k,-k} \Sigma_{-k,-k}^{-1} \Sigma_{-k,k}$, and Cholesky factors \mathbf{L}_k , with $\mathbf{L}_k \mathbf{L}_k^T = \Sigma_{k,k} - \Sigma_{k,-k} \Sigma_{-k,-k}^{-1} \Sigma_{-k,k}$, for each $k = 1, \dots, K$. By contrast, Gibbs samplers based on conditionally Gaussian representations (e.g., [Armagan, Clyde, and Dunson 2011](#)) have full conditional updates of the form

$$(\beta \mid \sigma^2, \mathbf{D}) \sim N((\mathbf{X}^T \mathbf{X} + \mathbf{D})^{-1} \mathbf{X}^T \mathbf{y}, \sigma^2 (\mathbf{X}^T \mathbf{X} + \mathbf{D})^{-1}), \quad (8)$$

which require costly Cholesky or eigenvalue decompositions of the matrix $(\mathbf{X}^T \mathbf{X} + \mathbf{D})^{-1}$ at each iteration as \mathbf{D} is updated—eliminating this step at each iteration is the primary savings of the new algorithm. From this basic observation, two notable facts follow:

1. Because the efficiency of our sampler relies on precomputing these statistics, it is not immediately applicable to regression models that require data augmentation at the observation level, such as models allowing non-Gaussian errors via mixtures of normals (e.g., t -distributed errors as scale-mixture of normals or location mixtures for multi-modal error distributions). For such expanded models, the analogous expressions involve latent parameters that vary across sampling iterations. It is possible that our slice sampler could be modified for non-Gaussian errors, but the extension would not be straightforward and we do not consider it further here.
2. Parallelization improves the traditional Gibbs sampler more than it improves the elliptical slice sampler. Note that computation of (7) can be improved with parallelization of linear algebra routines, meaning that this improvement is realized in each iteration. By contrast, the slice sampler can parallelize the precomputation of the conditional distributions, but this is a one-time upfront benefit. Accordingly, comparisons between the new slice sampling approach and the traditional samplers will depend on whether or not parallelization is used, such as via the efficient Math Kernel Library (MKL) linear algebra library. Some of our simulations use MKL

Algorithm 2 : *Slice-within-Gibbs sampler for linear regression*

- For each k from 1 to K
 - Update $\beta^k | \beta^{\{-k\}}, \sigma^2, \lambda$ according to Algorithm 1.
 1. Construct the conditional mean $\tilde{\beta}^k$ and conditional covariance matrix $\tilde{\Sigma}^k$ as in expressions (5) and (6). Set $\Delta^k = \beta^k - \tilde{\beta}^k$. Draw $v \sim N(0, \tilde{\Sigma}^k)$. Set $v_0 = \Delta^k \sin \theta^k + v \cos \theta^k$ and $v_1 = \Delta^k \cos \theta^k - v \sin \theta^k$.
 2. Draw ℓ uniformly on $[0, \pi(\Delta^k + \tilde{\beta}^k)]$. Initialize $a = 0$ and $b = 2\pi$.
 - (a) Sample θ' uniformly on $[a, b]$.
 - (b) If $\pi(\tilde{\beta}^k + v_0 \sin \theta' + v_1 \cos \theta') > \ell$, set $\theta^k \leftarrow \theta'$. Otherwise, shrink the support of θ' (if $\theta' < \theta^k$, set $a \leftarrow \theta'$; if $\theta' > \theta^k$, set $b \leftarrow \theta'$), and go to step (a).
 3. Return $\Delta^k = v_0 \sin \theta^k + v_1 \cos \theta^k$ and $\beta^k = \tilde{\beta}^k + \Delta^k$.
 - Update $\sigma^2 | \beta, \lambda$: let $s = (y - \mathbf{X}\beta)^T (y - \mathbf{X}\beta)$. Draw $\sigma^2 \sim \text{IG}((n+\alpha)/2, (s+\gamma)/2)$, where IG denotes the inverse-gamma distribution and (α, γ) are the associated prior parameters.
 - Update $\lambda | \beta, \sigma^2$ via a random walk Metropolis-Hastings step on the log scale with a diffuse Gaussian prior:
 1. Draw $r \sim N(0, 0.2^2)$, let $\lambda_{\text{proposal}} = \exp(\log(\lambda) + r)$.
 2. Compute the Metropolis-Hastings ratio

$$\eta = \exp(\log \pi(\beta, \lambda_{\text{proposal}}) - \log \pi(\beta, \lambda) + \log(\lambda_{\text{proposal}}) - \log(\lambda)) \quad (7)$$
 3. Draw $u \sim \text{Unif}(0, 1)$, if $u < \eta$, accept $\lambda_{\text{proposal}}$; otherwise keep the current λ .

Figure 2. The full slice-within-Gibbs sampler, including update steps for σ^2 and λ .

and some do not, but we clearly indicate in each caption whether parallelization has been employed. Figure 3 shows the impact of additional processors on the performance comparison using effective sample size per second (as defined in Section 3.3).

Finally, although the slice approach may incur additional computational cost if many proposals are rejected in each iteration prior to acceptance, we find that not to be the case. Figure 4 plots the average number of rejections before one accepted draw against average running time under different signal-to-noise ratios. When signal-to-noise ratio is high, the likelihood is strong, thus the elliptical slice sampler rejects fewer proposals and is accordingly faster. For signal-to-noise ratios between 1 and 4, the expected number of rejections is approximately constant.

2.5. The Rank-Deficient Case

It is increasingly common to want to analyze regression models with more predictors than observations: $p > n$. Similarly, it is sometimes the case that $\mathbf{X}^T \mathbf{X}$ can be rank-deficient due to perfect collinearity in the predictor matrix \mathbf{X} . Such cases would seem to pose a problem for our method for the

following reason. Recall that the slice sampler draws from a target distribution of the form

$$p(\beta | y, \mathbf{X}, \sigma) \propto N_Y(\mathbf{X}\beta, \sigma^2)\pi(\beta) \propto N_\beta(\hat{\beta}, \sigma^2(\mathbf{X}^T \mathbf{X})^{-1})\pi(\beta), \quad (9)$$

where we abuse notation somewhat and use $N(\cdot, \cdot)$ to denote the Gaussian distribution function. If $\text{rank}(\mathbf{X}^T \mathbf{X}) = r < p$, then the first term on the right-hand side is not absolutely continuous with respect to the second term, and the sampler will not function properly. Intuitively, the proposal distribution is supported on an $r < p$ dimensional hyperplane. The slice sampler will never propose values off of this subspace; hence it cannot have the correct target distribution. Operationally, $\hat{\beta}$ is not even unique. Fortunately, the algorithm can be salvaged with a very minor modification inspired by ridge regression analysis. We rewrite the above expression as

$$p(\beta | y, \mathbf{X}, \sigma) \propto N_Y(\mathbf{X}\beta, \sigma^2)N_\beta(0, c\sigma^2\mathbf{I})\frac{\pi(\beta)}{N_\beta(0, c\sigma^2\mathbf{I})}, \propto N_\beta(\bar{\beta}, \sigma^2(\mathbf{X}^T \mathbf{X} + c^{-1}\mathbf{I})^{-1})\frac{\pi(\beta)}{N_\beta(0, c\sigma^2\mathbf{I})}, \quad (10)$$

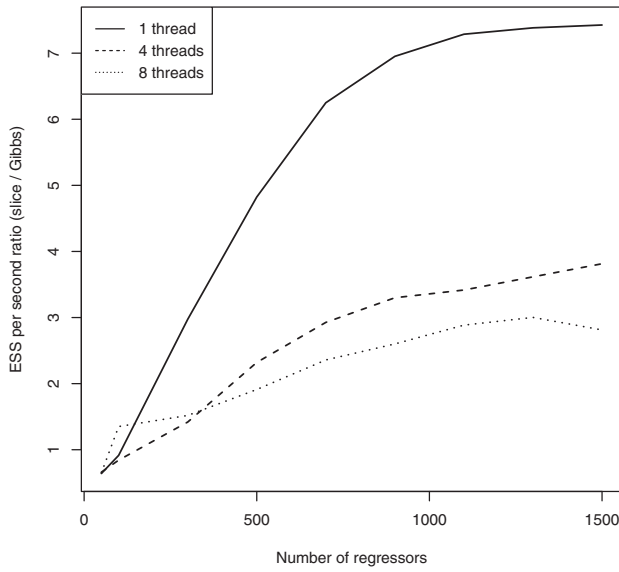


Figure 3. Ratio of effective sample size per second of the elliptical slice sampler and `monomvn` Gibbs sampler with different numbers of regressors and numbers of threads used in parallel. The ratio increases, indicating that the elliptical slice sampler is faster, with the number of regressors, but decreases as the number of threads increases because the MKL library improves the performance of the `monomvn` package. However, the elliptical slice sampler is still much faster than Gibbs sampler.

for $c > 0$, where $\bar{\beta} = (\mathbf{X}^T \mathbf{X} + c^{-1} \mathbf{I})^{-1} \mathbf{X}^T \mathbf{y}$. In the first line we merely “multiplied by 1;” subsequent lines reorganize the distributions in the familiar form required by the slice sampler. This reformulation solves the problem of absolute continuity; $\bar{\beta}$ is now well-defined and $(\mathbf{X}^T \mathbf{X} + c^{-1} \mathbf{I})$ is full rank. Otherwise, the algorithm operates exactly as before, only feeding in $\bar{\beta}$ rather than $\hat{\beta}$ and $(\mathbf{X}^T \mathbf{X} + c^{-1} \mathbf{I})$ rather than $\mathbf{X}^T \mathbf{X}$ and evaluating the ratio $\pi(\beta)/N(0, c\sigma^2 \mathbf{I})$ where one would have otherwise evaluated the prior $\pi(\beta)$. The optimal value of c will differ depending on the data and the prior being used; in practice small values near one seem to work fine, but tuning based on pilot runs could be performed if desired.

3. Simulation Studies

In this section, we compare the performance of our new algorithm against several well-known alternatives. Specifically, we

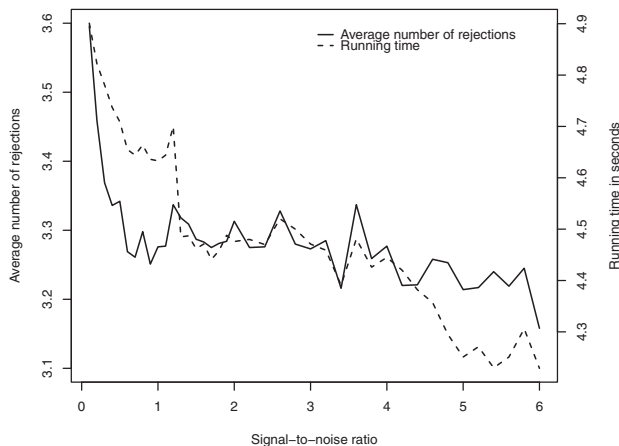


Figure 4. Average number of rejections in each iteration prior to acceptance and raw computing time over a range of signal-to-noise ratios. Here, we show the result of horseshoe regression with $p = 100$ and $n = 1000$, drawing 12,000 posterior samples.

apply our approach to the horseshoe prior (Carvalho, Polson, and Scott 2010), the Laplace prior (Park and Casella 2008; Hans 2009), and the independent Gaussian or “ridge” prior. These three priors are frequently used in empirical studies in part because they have readily available implementations.

The goal here is merely to demonstrate the efficacy of our computational approach, not to advocate for any particular prior choice. Indeed, our hope is that having a generic sampling scheme for any prior will make computational considerations secondary when choosing one’s prior. Ideally, one would not select a prior merely on the grounds that it admits an efficient sampling algorithm. In other words, the selling point of the present approach is not that it is strictly better than the existing samplers for these models (it is not necessarily), rather it is that we are using the *same* underlying algorithm for all three of them, with no custom modifications, and are still achieving competitive (or superior) computational performance. In the $p > n$ regime, we also compare to the recent algorithm of Johndrow, Orenstein, and Bhattacharya (2017); default Gibbs samplers were too costly time-wise to conduct simulations for $p > 500$. In the following subsections, we detail the priors considered as well as our data-generating process.

3.1. Priors

We investigate three standard priors: the horseshoe prior (Carvalho, Polson, and Scott 2010), the Laplace prior (Park and Casella 2008; Hans 2009), and the conjugate Gaussian prior (ridge regression). Details of these priors are provided here for reference.

Horseshoe prior. The horseshoe prior can be expressed as a local scale-mixture of Gaussians

$$\beta \sim N(0, \lambda^2 \Lambda^2), \quad \lambda \sim C^+(0, 1), \quad \lambda_1, \dots, \lambda_p \stackrel{\text{iid}}{\sim} C^+(0, 1), \quad (11)$$

where $C^+(0, 1)$ is a half-standard Cauchy distribution, $\Lambda = \text{diag}(\lambda_1, \dots, \lambda_p)$ represents the local shrinkage parameters and λ is the global shrinkage parameter. The standard approach to sampling from the posterior of regressions under horseshoe priors is a Gibbs sampler which samples $(\lambda_1, \dots, \lambda_p)$ from their full conditionals.

The horseshoe density, integrating over the local scale factors λ_j , can be computed using special functions. However, the following bounds (Carvalho, Polson, and Scott 2010) provide an excellent approximation which is more straightforward to evaluate:

$$\begin{aligned} \frac{1}{2\sqrt{2\pi^3}} \log \left(1 + \frac{4}{(\beta_j/\lambda)^2} \right) &< \pi(\beta_j/\lambda) \\ &< \frac{1}{\sqrt{2\pi^3}} \log \left(1 + \frac{2}{(\beta_j/\lambda)^2} \right). \end{aligned} \quad (12)$$

In our implementation, we use the lower bound as our prior density function.

Laplace prior. The Laplace (double-exponential) prior is given by

$$\pi(\beta_j | \lambda) = \frac{1}{2} \lambda^{-1} \exp(-|\beta_j|/\lambda). \quad (13)$$

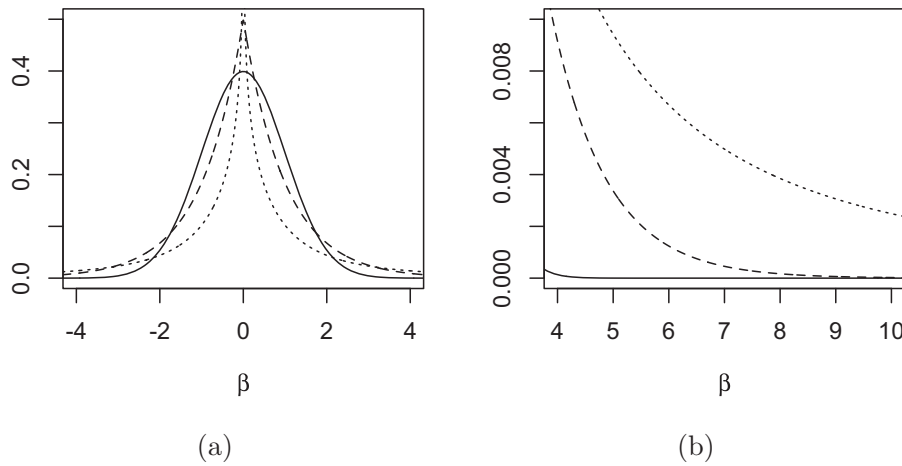


Figure 5. Three priors for regression coefficients: Gaussian (solid), Laplace (dashed), horseshoe (dotted) when $\lambda = 1$. Panel (a) shows the body of the distributions and panel (b) shows a zoomed-in look at the tails.

Park and Casella (2008) gave the first treatment of Bayesian lasso regression and Hans (2009) proposed the alternative Gibbs samplers.

Ridge prior. The ridge prior is given by

$$\beta \mid \lambda \sim N(0, \lambda^2 \mathbf{I}_p). \tag{14}$$

Section 2.3.2 of Gamerman and Lopes (2006) provides a nice exposition of the general Bayesian linear and Gaussian regression model.

Note that all three priors have a “global” shrinkage parameter λ , which is given a hyperprior. A key feature of Bayesian shrinkage regression is the inference of this parameter; as opposed to setting it at a fixed value or selecting it by cross-validation, point estimates of β are obtained as the marginal posterior mean, integrating over (the posterior of) λ . Figure 5 plots these three densities for comparison.

3.2. Data-Generating Process

The predictor matrix \mathbf{X} is generated in two different ways: independently from a standard Gaussian distribution, or according to a Gaussian factor model so that variables have strong linear codependencies. Details of the data-generating process are shown below.

1. Draw elements of β from a “sparse Gaussian” where $[p]$ entries of β are nonzero, drawn from a standard Gaussian distribution, and all other entries are zero.
2. Generate the regressors matrix \mathbf{X} in one of two ways.
 - In the independent regressor case, every element of the regressor matrix $\mathbf{X}_{n \times p}$ is drawn independently from a standard Gaussian distribution.
 - In the factor structure case, we draw each row of \mathbf{X} from a Gaussian factor model with $k = p/5$ factors. Latent factor scores are drawn according to $\mathbf{F}_{k \times n} \sim N(0, 1)$. The factor loading matrix, $\mathbf{B}_{p \times k}$, has entries that are either zero or one, with exactly five ones in each column and a single 1 in each row, so that $\mathbf{B}\mathbf{B}^T$ is block diagonal, with blocks of all ones and all other elements being zero. The regressors are then set as $\mathbf{X} = (\mathbf{B}\mathbf{F})^T + \boldsymbol{\varepsilon}$ where $\boldsymbol{\varepsilon}$ is an $n \times p$ matrix of errors with independent $N(0, 0.01)$ entries.

3. Set $\sigma = \kappa \sqrt{\sum_{j=1}^p \beta_j^2}$, where κ controls noise level.
 4. Draw $y_i = \mathbf{x}_i' \beta + \epsilon_i$, $\epsilon_i \sim N(0, \sigma^2)$ for $i = 1, \dots, n$.
- Additionally, we vary the noise level, letting $\kappa = 1$ or $\kappa = 2$, corresponding to signal-to-noise ratios of 1 and 1/2, respectively.

3.3. Comparison Metrics

To gauge the performance of our new algorithm, we must judge not only the speed, but also the quality of the posterior samples. To address this concern, we compare our approach with alternative samplers using effective sample size per second (see, e.g., Gamerman and Lopes 2006, pp. 126–127). Letting N denote the Monte Carlo sample size, the effective sample size $N_{\text{eff}}(\beta_j)$ is

$$N_{\text{eff}}(\beta_j) = \frac{N}{1 + 2 \sum_{k=1}^{\infty} \rho_k}, \tag{15}$$

where $\rho_k = \text{corr}(\beta_j^{(0)}, \beta_j^{(k)})$ is the autocovariance of lag k . To verify that the samplers are giving comparable results (they ought to be fitting the same model), we also report the estimation error of the associated posterior point estimates. Suppose $\{\bar{\beta}_j\}$ are posterior means of each variable and $\{\beta_j\}$ are true values. The estimation error is measured by

$$\text{error} = \sqrt{\frac{\sum_{j=1}^p (\bar{\beta}_j - \beta_j)^2}{\sum_{j=1}^p \beta_j^2}}. \tag{16}$$

Although we do not report it here, we also examined posterior standard deviations and found all algorithms to be comparable up to Monte Carlo error. For each simulation, 50,000 posterior samples are drawn, 20,000 of which are burn-in samples (with no thinning). We divide N_{eff} by running time in seconds to compute ESS per second as a measure of efficiency of each sampler.

3.4. Simulation Study Results

The R package `monomvn` (Gramacy 2017) implements the standard Gibbs samplers for the horseshoe prior (function `bhS`), the Laplace prior (function `blasso`), and Gaussian prior (function `bridge`) prior. For the Laplace prior, we additionally compare with the Gibbs sampler from Hans (2009). All of the samplers

Table 1. Simulation results of all three priors, where $\kappa = 1$ and all regressors are independent. The table demonstrates error and effective sample size per second of the elliptical slice sampler, Gibbs sampler in R package `monomvn` (column `monomvn`), and our own implementation of Gibbs sampler for horseshoe regression (column `Gibbs`). The elliptical slice sampler has similar error to the Gibbs sampler, but much higher effective sample size per second.

Prior	p	n	Error				ESS per second		
			OLS	slice	monomvn	Gibbs	slice	monomvn	Gibbs
Horseshoe	100	10p	3.38%	1.52%	1.51%	1.51%	1399	613	567
	1000	10p	1.05%	0.27%	0.27%	0.27%	91	5	5
Laplace	100	10p	3.38%	2.39%	2.38%	—	2362	809	—
	1000	10p	1.04%	0.63%	0.63%	—	168	8	—
Ridge	100	10p	3.38%	3.20%	3.20%	—	3350	959	—
	1000	10p	1.06%	0.99%	0.99%	—	178	5	—

are implemented in C++. Tables 1 and 2 report a representative subset of our simulation results; comprehensive tables can be found in the Appendix. Here we summarize the broad trends that emerge.

First, the slice sampler enjoys a substantial advantage in terms of effective sample size (ESS) per second compared to the standard samplers. For example, in the independent regressor case (Table 1), when $p = 1000$ and $n = 10 \times p$, our approach is about 18 times faster than the `monomvn` Gibbs sampler.

When there exist strong colinearities in the regressor matrix (Table 2), the new approach, which samples one coefficient at a time, loses some of its efficiency compared to the standard algorithms, which draw the regression coefficients jointly. However, the new approach is still superior when $p > 1000$.

In addition to effective sample size per second, we also consider raw computing time. The code is tested on a machine with an Intel i7-6920HQ CPU and 16GB RAM. For the horseshoe regression with independent regressors, with $p = 500$ and $n = 5000$, the slice-within-Gibbs sampler takes 101 sec running time to draw 50,000 posterior samples, of which 19 sec are fixed computing time and 82 sec are spent within the loop. By comparison, the standard Gibbs sampler takes 1 sec of fixed computing time and 5310 sec within the loop to draw the same number of posterior samples.

3.4.1. The $p > n$ Setting

In the $p > n$ regime, we compare our algorithm to the sampler presented in Johndrow, Orenstein, and Bhattacharya (2017). (We are grateful to the authors for making their Matlab code available.) This choice was based on the fact that the standard Gibbs samplers are prohibitively slow for $p = 1000$, with a runtime of 1450 sec versus 92 sec when $n = 900$. Indeed, the infeasibility of existing methods for an applied dataset with $p = 1500$ and $n = 300,000$ was our initial motivation for developing the approach described in this article. The Johndrow, Orenstein, and Bhattacharya (2017) approach was developed

contemporaneously to our method, but focuses on the case where $p \gg n$ (such as genome-wide association studies).

First, we note that both methods give similar root mean squared error (RMSE), suggesting that the posteriors being sampled from are comparable. Second, the elliptical slice sampler scales well with n given a fixed p . For example, the ESS per second of our approach is around 40 when $p = 1000$ and n ranges from 300 to 900. By contrast, Johndrow, Orenstein, and Bhattacharya (2017) does well when $p \gg n$ such as when $p = 3000$ and $n = 100$; in that case its ESS per second is as high as 69. However, the ESS per second drops significantly when n becomes larger for their approach. A full comparison is displayed in Table 3.

4. Empirical Illustration: Beauty and Course Evaluations

In this section, we consider an interesting dataset first presented in Hamermesh and Parker (2005). The data are course evaluations from the University of Texas at Austin between 2000 and 2002. The data are on a 1 to 5 scale, with larger numbers being better. In addition to the course evaluations, information concerning the class and the instructor were collected. To quote Hamermesh and Parker (2005):

We chose professors at all levels of the academic hierarchy, obtaining professorial staffs from a number of departments that had posted all faculty members' pictures on their departmental websites. An additional ten faculty members' pictures were obtained from miscellaneous departments around the University. The average evaluation score for each undergraduate course that the faculty member taught during the academic years 2000–2002 is included. This sample selection criterion resulted in 463 courses, with the number of courses taught by the sample members ranging from 1 to 13. The classes ranged in size from 8 to 581 students, while the number of students completing the instructional ratings ranged from 5 to 380. Underlying the 463 sample observations are 16,957 completed evaluations from 25,547 registered students.

Table 2. Simulation results of all three priors, $\kappa = 1$.

Prior	p	n	Error				ESS per second		
			OLS	1-block	monomvn	Gibbs	1-block	monomvn	Gibbs
Horseshoe	100	10p	16.47%	6.06%	6.04%	6.03%	387	747	792
	1000	10p	6.85%	1.64%	1.64%	1.64%	36	4	4
Laplace	100	10p	17.06%	7.21%	7.15%	—	573	1257	—
	1000	10p	6.77%	1.95%	1.94%	—	38	5	—
Ridge	100	10p	16.90%	8.50%	8.75%	—	669	1668	—
	1000	10p	6.85%	2.93%	3.09%	—	38	6	—

NOTES: The regressors are not independent but have underlying factor structure, in that every five regressors are highly correlated with one another. The elliptical slice sampler has similar error to the Gibbs sampler, but much higher effective sample size per second when $p = 1000$.

Table 3. Comparison of effective sample size (ESS) per second and root mean squared error (RMSE) with Johndrow, Orenstein, and Bhattacharya (2017) (denoted J&O) for the $p > n$ case. Both samplers take 12,000 posterior draws with the first 2000 as burn-in. Both samplers give similar RMSE. The elliptical slice sampler has higher ESS per second in most cases considered here, especially when $p \approx n$. The Johndrow et al. sampler is much more efficient only when $p \gg n$, such as $p = 3000$ and $n = 100$. Results were tabulated *without* the MKL linear algebra library.

p	n	κ	Running time		RMSE		ESS per second	
			J&O	Slice	J&O	Slice	J&O	Slice
1000	300	0.25	119.11	91.50	0.0041	0.0038	46.71	43.19
1000	600	0.25	394.02	88.61	0.0028	0.0026	14.68	47.26
1000	900	0.25	905.36	88.91	0.0021	0.0020	6.60	48.85
1000	300	1	127.33	90.19	0.0189	0.0189	43.92	39.25
1000	600	1	399.50	91.17	0.0129	0.0129	14.39	44.12
1000	900	1	927.96	91.58	0.0098	0.0099	6.35	46.09
1500	450	0.25	346.37	187.91	0.0029	0.0027	16.37	21.26
1500	900	0.25	1073.28	185.57	0.0022	0.0021	5.50	23.08
1500	1350	0.25	2629.52	183.68	0.0018	0.0017	2.27	24.04
1500	450	1	326.63	183.66	0.0164	0.0164	17.39	20.28
1500	900	1	1021.47	174.52	0.0100	0.0101	5.73	23.72
1500	1350	1	2515.37	176.51	0.0071	0.0071	2.36	24.78
3000	100	0.25	85.95	985.68	0.0067	0.0075	69.72	3.89
3000	500	0.25	575.92	983.64	0.0024	0.0022	9.85	4.17

For additional details on how the beauty scores were constructed and on how to interpret the regression results, see Hamermesh and Parker (2005). Here, we do not aim to provide any sort of definitive reanalysis of the results in Hamermesh and Parker (2005). Instead, our goal is to fit a plausible, but over-parameterized, model to their data and to employ a variety of priors, including some nonstandard priors in addition to the usual shrinkage priors (horseshoe, Laplace, and ridge). We are interested in finding out whether conclusions change substantively under “exotic” priors that are not likely to be used by the typical social scientist.

The model we fit allows for fixed effects for each of 95 instructors. (We recover the instructors by matching on teacher characteristics, including a variable denoting if the professor’s photo is in black and white or in color. Using this method we find 95 uniques, although the original article says there are 94 instructors. The data we used can be found at <http://faculty.chicagobooth.edu/richard.hahn/teaching/hamermesh.txt>.) We include additive effects for the following factors: class size (number of students), language in which the professor earned his or her degree, whether or not the instructor was a minority, gender, beauty rating, and age. Each of these variables was included in the model via dummy variables according to the following breakdown:

- class size: below 31, 31 to 60, 61 to 150, or 151 to 600 (four levels by quartile),
- language: English or non-English (two levels),
- minority: ethnic minority or nonminority (two levels),
- gender: male or female (two levels),
- beauty: four levels by quartile, and
- age: below 43, 43 to 47, 48 to 56, and 57 to 73 (four levels by quartile).

Finally, we include up to three-way interactions between age, beauty, and gender. We include an intercept in our model so that individual effects can be interpreted as deviation from the average. Three predictors are then dropped because they are collinear with the intercept (and each other); there were no highly beautiful males between 42 and 46, and no moderately beautiful instructors of either gender in that same age group. Even after dropping these columns, the model is numerically

singular, with only 98 out of 130 singular values greater than $1e-14$.

In addition to the horseshoe, Laplace, and ridge regression priors, we also analyze these data using two exotic priors: an asymmetric Cauchy prior and a “nonlocal” two-component mixture of Cauchys.

The asymmetric Cauchy prior is

$$\pi(\beta) = \begin{cases} 2qf(\beta) & \beta \leq 0 \\ 2f(\beta/s)(1-q)/s & \beta > 0 \end{cases}, \quad (17)$$

where $f(x) = \frac{1}{\pi(1+x^2)}$ is the density of the standard Cauchy distribution and $s = (1-q)/q$. Here, q is the prior probability that the coefficient is negative. We refer to this prior as having a shark fin density, as suggested by the shape shown in Figure 6. The bivariate mixture of Cauchys prior is

$$\pi(\beta) = 0.5t(\beta; -1.5, 1) + 0.5t(\beta; 1.5, 1), \quad (18)$$

where $t(x; m, v)$ is the density of the Student- t distribution with location m and degrees of freedom v . The nonlocal mixture of Cauchys is a sort of “anti-sparsity” prior: it asserts that the coefficients are all likely to be similar in magnitude and nonzero, but with unknown sign. A global scale parameter can be accommodated within the above forms by using density $\pi(\beta/\lambda)/\lambda$. Figure 6 displays the density functions of these two priors.

When applying the exotic priors to the course evaluations model, we differentiated between regressors in terms of hyperparameter selection. Specifically, in the asymmetric Cauchy model we defaulted to $q = 0.5$, except for the following: for the largest class size, we set $q = 0.75$, for tenure track status we set $q = 0.25$, for non-English we set $q = 0.75$, and for each of the three higher beauty levels we set $q = 0.25$. Similarly, for the nonlocal Cauchy mixture, we defaulted to a standard Cauchy, using the nonlocal prior only for the class size, tenure track, language, and minority variables.

Our results are summarized in Table 4, which reports all variables whose posterior 95% quantile-based symmetric credible interval excluded zero for at least one of the five priors. Figure 7 shows kernel density plots of posterior samples of these coefficients. All posterior inferences were based on effective sample

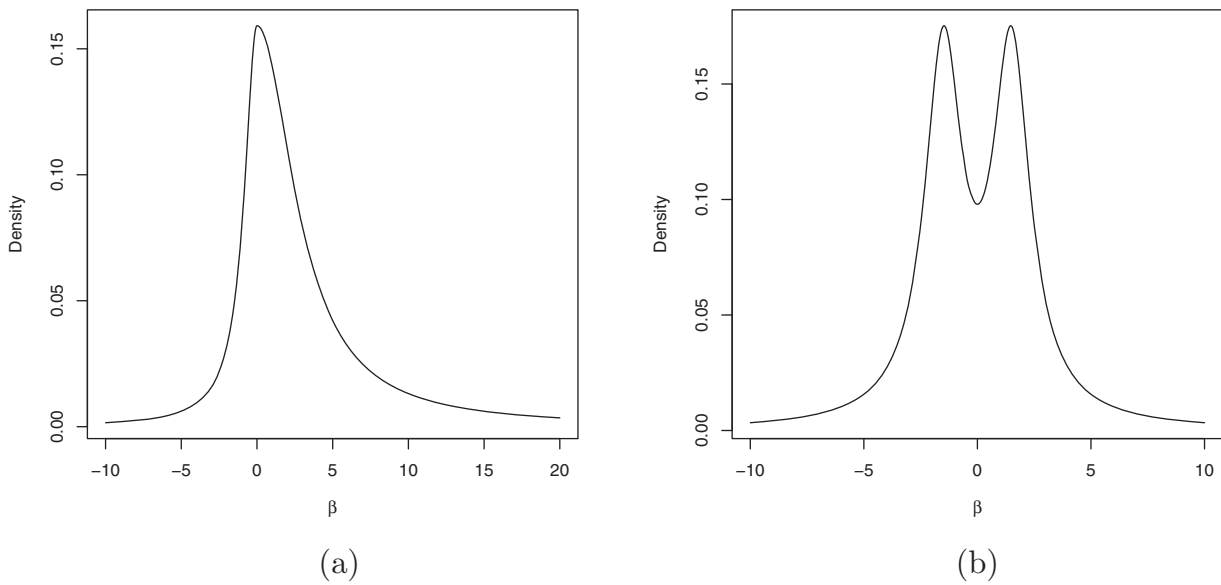


Figure 6. Panel (a) depicts the density of the “shark fin” prior with $q = 0.25$. Panel (b) depicts the density of a two-component Cauchy mixture distribution where the weight for each component is $1/2$, the scale parameter is 1, and the location parameters are -1.5 and 1.5 , respectively.

sizes of approximately 20,000. A number of features stand out. First, there is a relatively small set of factors that are isolated between the various models as statistically significant (in the Bayesian sense described above); this suggests that the data are meaningfully overwhelming the contributions of the priors. Likewise, we note that the signs on the point estimates concur

across all five priors. Second, we note that different priors do make a difference, both in terms of which variables among this set are designated significant and also in terms of the magnitude of the point estimates obtained. Third, one specific difference in the results that is noteworthy is that the horseshoe prior does not flag beauty as significant, while the ridge prior gives a much

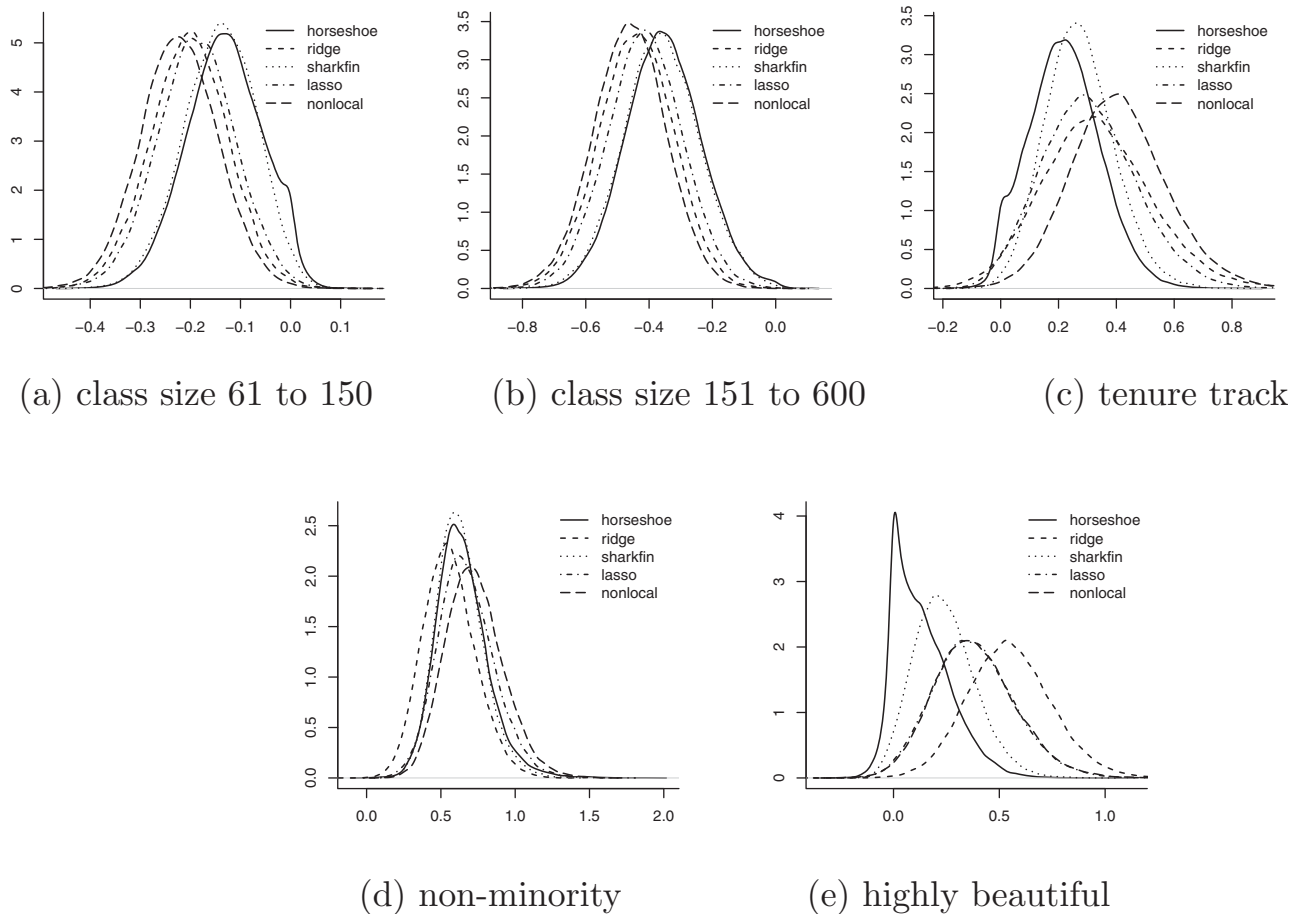


Figure 7. Kernel density plots of posterior samples of regression coefficients.

Table 4. Posterior points estimates of regression coefficients under each prior; those whose posterior 95% credible intervals exclude zero are shown in bold.

Variable name	Horseshoe	Lasso	Ridge	Sharkfin	Nonlocal
Class size 61 to 150	-0.13	-0.19	-0.20	-0.14	-0.22
Class size 151 to 600	-0.36	-0.41	-0.43	-0.36	-0.46
Tenure track	0.22	0.29	0.31	0.27	0.40
Nonminority	0.65	0.65	0.53	0.63	0.71
Highly beautiful	0.14	0.36	0.54	0.25	0.38

larger estimate. In Figure 7, the horseshoe posterior (black line) appears notably different than the other priors in panel (e), exhibiting bimodality, where one mode is at 0 and another mode is located away from zero in the direction of the maximum likelihood estimate; this distinctive shape is consistent with the horseshoe prior’s aggressive shrinkage profile at the origin.

5. Discussion

This article presents a new and efficient sampler for the purpose of Bayesian linear regression with arbitrary priors. The new method is seen to be competitive with, or better than, the usual Gibbs samplers that are routinely used to fit such models using

popular shrinkage priors. The new approach is flexible enough to handle any class of priors admitting density evaluations. We hope that our new sampling approach will foster research into interesting classes of priors that do not have obvious latent variable representations and to encourage empirical researchers to conduct more bespoke sensitivity analysis.

Appendix: Complete Simulation Results

In the appendix, we show complete simulation results. The data-generating process is presented in Section 3.2 We implement the elliptical slice sampler for horseshoe, Laplace, and ridge priors, and compare with the monomvn package for all three priors, Hans (2009) for the Laplace prior, and our own implementation of the Gibbs sampler for the horseshoe prior. Numerical results are reported in tables A.1 through A.7.

A1. Independent Regressors

In this section, all elements of the regressor matrix $X_{n \times p}$ are drawn independently from a standard Gaussian distribution. The regression coefficients β are drawn from a sparse Gaussian data-generating process as shown in Section 3.2 κ controls the noise level. All simulations for independent regressors are on machines without the Math Kernel Library (MKL).

A1.1. Horseshoe Prior

Table A.1. This table compares the error and effective sample size (ESS) per second of various sampling algorithms under the horseshoe prior.

p	n	Error				ESS per second		
		OLS	slice	monomvn	Gibbs	slice	monomvn	Gibbs
100	10p	3.379%	1.519%	1.514%	1.514%	1399	613	567
100	50p	1.414%	0.655%	0.655%	0.654%	1871	517	670
100	100p	1.007%	0.464%	0.464%	0.463%	1500	301	590
500	10p	1.493%	0.439%	0.441%	0.439%	229	29	31
500	50p	0.637%	0.196%	0.196%	0.196%	228	20	30
500	100p	0.451%	0.143%	0.143%	0.143%	215	10	17
1000	10p	1.050%	0.269%	0.269%	0.270%	91	5	5
1000	50p	0.448%	0.113%	0.113%	0.113%	76	3	3
1000	100p	0.317%	0.081%	0.081%	0.081%	74	2	3

NOTES: The signal-to-noise ratio is $\kappa = 1$, and the response variable is drawn according to the sparse Gaussian model described in the main text. All regressors are mutually independent. Observe that the monomvn package is notably less efficient than our implementation of the Gibbs sampler. We believe this is because monomvn allows t -distributed errors, which demands recomputing the sufficient statistics at each iteration, leading it to scale poorly in n . This table was generated on a machine *not* running the MKL linear algebra library.

Table A.2. This table compares the error and effective sample size (ESS) per second of various sampling algorithms under the horseshoe prior.

p	n	Error				ESS per second		
		OLS	slice	monomvn	Gibbs	slice	monomvn	Gibbs
100	10p	6.846%	2.990%	2.989%	2.981%	1248	438	525
100	50p	2.784%	1.348%	1.340%	1.339%	1499	348	588
100	100p	1.989%	0.884%	0.883%	0.883%	1616	331	619
500	10p	2.999%	0.945%	0.945%	0.946%	236	21	20
500	50p	1.286%	0.412%	0.413%	0.412%	249	15	20
500	100p	0.899%	0.275%	0.275%	0.275%	260	12	20
1000	10p	2.121%	0.550%	0.550%	0.551%	79	4	4
1000	50p	0.912%	0.245%	0.245%	0.245%	92	4	6
1000	100p	0.639%	0.172%	0.172%	0.172%	89	3	6

NOTES: The signal-to-noise ratio is $\kappa = 2$, and the response variable is drawn according to the sparse Gaussian model described in the main text. All regressors are mutually independent. Observe that the monomvn package is notably less efficient than our implementation of the Gibbs sampler. We believe this is because monomvn allows t -distributed errors, which demands recomputing the sufficient statistics at each iteration, leading it to scale poorly in n . This table was generated on a machine *not* running the MKL linear algebra library.

A1.2. Laplace Prior

Table A.3. This table compares the error and effective sample size (ESS) per second of various sampling algorithms under a Laplace prior.

p	n	Error				ESS per second		
		OLS	slice	monomvn	Hans	slice	monomvn	Hans
100	10 p	3.378%	2.385%	2.383%	2.419%	2362	809	1160
100	50 p	1.436%	1.183%	1.182%	1.193%	3657	696	1202
100	100 p	1.017%	0.869%	0.869%	0.875%	3870	646	1257
500	10 p	1.493%	0.955%	0.956%	0.958%	472	48	131
500	50 p	0.639%	0.491%	0.490%	0.495%	482	19	149
500	100 p	0.447%	0.364%	0.364%	0.370%	508	16	173
1000	10 p	1.041%	0.629%	0.627%	0.631%	168	8	78
1000	50 p	0.451%	0.333%	0.333%	0.333%	156	4	85
1000	100 p	0.317%	0.249%	0.249%	0.249%	144	3	82

NOTES: The signal-to-noise ratio is $\kappa = 1$, and the response variable is drawn according to the sparse Gaussian model described in the main text. All regressors are mutually independent. The ratio column reports the ratio of ESS per second for elliptical slice sampler and that of `monomvn` package. This table was generated on a machine *not* running the MKL linear algebra library.

Table A.4. This table compares the error and effective sample size (ESS) per second of various sampling algorithms under a Laplace prior.

p	n	Error				ESS per second		
		OLS	slice	monomvn	Hans	slice	monomvn	Hans
100	10 p	6.538%	3.990%	3.985%	3.991%	2203	682	1531
100	50 p	2.839%	2.100%	2.096%	2.103%	3034	662	1487
100	100 p	1.966%	1.539%	1.537%	1.537%	3209	370	1559
500	10 p	2.972%	1.586%	1.586%	1.590%	421	47	185
500	50 p	1.279%	0.858%	0.858%	0.857%	398	21	191
500	100 p	0.908%	0.654%	0.654%	0.654%	524	17	187
1000	10 p	2.105%	1.057%	1.054%	1.056%	156	5	63
1000	50 p	0.909%	0.585%	0.585%	0.586%	176	4	66
1000	100 p	0.641%	0.446%	0.446%	0.446%	171	4	61

NOTES: The signal-to-noise ratio is $\kappa = 2$, and the response variable is drawn according to the sparse Gaussian model described in the main text. All regressors are mutually independent. The ratio column reports the ratio of ESS per second for elliptical slice sampler and that of `monomvn` package. This table was generated on a machine *not* running the MKL linear algebra library.

A1.3. Ridge Regression

Table A.5. This table compares the error and effective sample size (ESS) per second of various sampling algorithms under a ridge prior.

p	n	Error			ESS per second		
		OLS	slice	monomvn	slice	monomvn	ratio
100	10 p	3.375%	3.197%	3.198%	3350	959	3.49
100	50 p	1.415%	1.399%	1.398%	4714	741	6.36
100	100 p	1.019%	1.012%	1.015%	4720	558	8.46
500	10 p	1.496%	1.418%	1.418%	534	28	19.07
500	50 p	0.642%	0.636%	0.636%	665	22	30.22
500	100 p	0.451%	0.447%	0.447%	645	17	37.94
1000	10 p	1.056%	0.992%	0.993%	178	5	35.60
1000	50 p	0.451%	0.446%	0.446%	213	4	53.25
1000	100 p	0.317%	0.315%	0.315%	228	4	57

NOTES: The signal-to-noise ratio is $\kappa = 1$, and the response variable is drawn according to the sparse Gaussian model described in the main text. All regressors are mutually independent. The ratio column reports the ratio of ESS per second for elliptical slice sampler and that of `monomvn` package. This table was generated on a machine *not* running the MKL linear algebra library.

Table A.6. This table compares the error and effective sample size (ESS) per second of various sampling algorithms.

p	n	Error			ESS per second		
		OLS	slice	monomvn	slice	monomvn	ratio
100	10 p	6.851%	5.735%	5.735%	2810	1145	2.45
100	50 p	2.853%	2.756%	2.757%	4240	776	5.46
100	100 p	2.078%	2.043%	2.043%	4000	636	6.29
500	10 p	2.984%	2.453%	2.459%	516	33	15.64
500	50 p	1.290%	1.236%	1.236%	730	26	28.08
500	100 p	0.892%	0.875%	0.875%	693	24	28.88
1000	10 p	2.098%	1.722%	1.726%	182	6	30.33
1000	50 p	0.904%	0.867%	0.868%	237	7	35.86
1000	100 p	0.642%	0.629%	0.629%	244	5	48.80

NOTES: The signal-to-noise ratio is $\kappa = 2$, and the response variable is drawn according to the sparse Gaussian model described in the main text. All regressors are mutually independent. The ratio column reports the ratio of ESS per second for elliptical slice sampler and that of `monomvn` package. This table was generated on a machine not running the MKL linear algebra library.

A2. Factor Structure

In this simulation study, the regressor matrix $\mathbf{X}_{n \times p}$ is drawn with the factor structure shown in Section 3.2. All results are generated on machines running the MKL linear algebra library.

Table A.7. This table compares the error and effective sample size (ESS) per second for various sampling algorithms.

Prior	p	n	Error				ESS per second		
			OLS	slice	monomvn	Gibbs	slice	monomvn	Gibbs
Horseshoe	20	200	26.93%	14.67%	14.52%	14.53%	1626	7281	8395
	100	1000	16.47%	6.06%	6.04%	6.03%	387	747	792
	200	2000	14.58%	4.54%	4.54%	4.54%	203	183	187
	500	5000	10.05%	2.61%	2.61%	2.62%	57	16	17
	1000	10,000	6.85%	1.64%	1.64%	1.64%	36	4	4
Laplace	20	200	27.27%	16.31%	16.25%	—	2357	12875	—
	100	1000	17.06%	7.21%	7.15%	—	573	1257	—
	200	2000	14.56%	5.29%	5.20%	—	365	306	—
	500	5000	10.01%	3.13%	3.10%	—	84	27	—
	1000	10,000	6.77%	1.95%	1.94%	—	38	5	—
Ridge	20	200	27.36%	17.33%	17.34%	—	2399	22608	—
	100	1000	16.90%	8.50%	8.75%	—	669	1668	—
	200	2000	14.38%	6.42%	6.69%	—	342	362	—
	500	5000	9.90%	4.18%	4.40%	—	89	30	—
	1000	10,000	6.85%	2.93%	3.09%	—	38	6	—

NOTES: The regressors are generated with factor structure, with blocks of consecutive 20 variables having correlation 0.8 but independent from the other blocks. The response variable is generated according to the sparse Gaussian model described in the text. The column “Gibbs” denotes our own implementation of the standard Gibbs sampler for the horseshoe prior. In this table, generated on a machine running the MKL linear algebra library, `monomvn` achieves very high ESS per second when the data size is small, but is still less efficient than the elliptical slice sampler as sample size and dimensionality grows; see the discussion on parallelization in Section 2.4.

Funding

The authors gratefully acknowledge the Booth School of Business for support. The third author acknowledges the support of research fellowships from the CNPq and FAPESP, Brazil.

References

Armagan, A. (2009), “Variational Bridge Regression,” in *Artificial Intelligence and Statistics, Proceedings of Machine Learning Research* (volume 5), eds. D. van Dyk and M. Welling, Clearwater Beach, FL, pp. 17–24. [142]

Armagan, A., Clyde, M., and Dunson, D. B. (2011), “Generalized Beta Mixtures of Gaussians,” in *Advances in Neural Information Processing Systems*, pp. 523–531. [142,144]

Armagan, A., Dunson, D. B., and Lee, J. (2013), “Generalized Double Pareto Shrinkage,” *Statistica Sinica*, 23, 119–143. [142]

Bhattacharya, A., Pati, D., Pillai, N. S., and Dunson, D. B. (2015), “Dirichlet-Laplace Priors for Optimal Shrinkage,” *Journal of the American Statistical Association*, 110, 1479–1490. [142]

Caron, F., and Doucet, A. (2008), “Sparse Bayesian Nonparametric Regression,” in *Proceedings of the 25th International Conference on Machine Learning*, ACM, pp. 88–95. [142]

Carvalho, C. M., Polson, N. G., and Scott, J. G. (2010), “The Horseshoe Estimator for Sparse Signals,” *Biometrika*, 97, 465–480. [142,146]

Gamerman, D., and Lopes, H. F. (2006), *Markov Chain Monte Carlo: Stochastic Simulation for Bayesian Inference*, Boca Raton, FL: CRC Press. [147]

Gramacy, R. B. (2017), “`monomvn`: Estimation for Multivariate Normal and Student-t Data With Monotone Missingness,” R Package Version 1.9-7. [147]

Griffin, J. E., and Brown, P. J. (2010), “Inference With Normal-Gamma Prior Distributions in Regression Problems,” *Bayesian Analysis*, 5, 171–188. [142]

- (2011), “Bayesian Hyper-LASSOs With Non-Convex Penalization,” *Australian & New Zealand Journal of Statistics*, 53, 423–442. [142]
- Hahn, P. R., He, J., and Lopes, H. (2018), “Bayeslm: Efficient Sampling for Gaussian Linear Regression With Arbitrary Priors,” R Package Version 0.7.0. [142]
- Hamermesh, D. S., and Parker, A. (2005), “Beauty in the Classroom: Instructors’ Pulchritude and Putative Pedagogical Productivity,” *Economics of Education Review*, 24, 369–376. [148]
- Hans, C. (2009), “Bayesian Lasso Regression,” *Biometrika*, 96, 835–845. [142,146,147,151]
- Johndrow, J. E., Orenstein, P., and Bhattacharya, A. (2017), “Scalable MCMC for Bayes shrinkage Priors,” arXiv preprint, arXiv:1705.00841. [142,146,148]
- Murray, I., Adams, R. P., and MacKay, D. J. (2010), “Elliptical Slice Sampling,” in *JMLR Workshop and Conference Proceedings* (Vol. 9), JMLR, eds. Y. W. Teh and M. Titterton, Sardinia, Italy, pp. 541–548. [142,143]
- Neal, R.M.(2003), “Slice Sampling,” *Annals of Statistics*, 31, 705–767. [143]
- Neville, S. E., Ormerod, J. T., and Wand, M. (2014), “Mean Field Variational Bayes for Continuous Sparse Signal Shrinkage: Pitfalls and Remedies,” *Electronic Journal of Statistics*, 8, 1113–1151. [142]
- Park, T., and Casella, G. (2008), “The Bayesian Lasso,” *Journal of the American Statistical Association*, 103, 681–686. [142,146]
- Polson, N. G., and Scott, J. G. (2010), “Shrink Globally, Act Locally: Sparse Bayesian Regularization and Prediction,” in *Bayesian Statistics* (Vol. 9), eds. J. M. Bernardo, M. J. Bayarri, J. O. Berger, A. P. Dawid, D. Heckerman, A. F. M. Smith, and M. West, Oxford: Oxford University Press, pp. 501–538. [142]
- Polson, N. G., Scott, J. G., and Windle, J. (2014), “The Bayesian Bridge,” *Journal of the Royal Statistical Society, Series B*, 76, 713–733. [142]
- R Core Team (2017), *R: A Language and Environment for Statistical Computing*, Vienna, Austria: R Foundation for Statistical Computing. [142]